ELSEVIER

SCIENCE DIRECT

PHYSICS LETTERS B

Physics Letters B 597 (2004) 39–46

www.elsevier.com/locate/physletb

Direct measurements of the branching fractions for $D^0 \to K^- e^+ \nu_e$ and $D^0 \to \pi^- e^+ \nu_e$ and determinations of the form factors $f_+^K(0)$ and $f_+^\pi(0)$

BES Collaboration

M. Ablikim [a], J.Z. Bai [a], Y. Ban [j], J.G. Bian [a], X. Cai [a], J.F. Chang [a], H.F. Chen [o], H.S. Chen [a], H.X. Chen [a], J.C. Chen [a], Jin Chen [a], Jun Chen [f], M.L. Chen [a], Y.B. Chen [a], S.P. Chi [b], Y.P. Chu [a], X.Z. Cui [a], H.L. Dai [a], Y.S. Dai [q], Z.Y. Deng [a], L.Y. Dong [a], S.X. Du [a], Z.Z. Du [a], J. Fang [a], S.S. Fang [b], C.D. Fu [a], H.Y. Fu [a], C.S. Gao [a], Y.N. Gao [n], M.Y. Gong [a], W.X. Gong [a], S.D. Gu [a], Y.N. Guo [a], Y.Q. Guo [a], K.L. He [a], M. He [k], X. He [a], Y.K. Heng [a], H.M. Hu [a], T. Hu [a], L. Huang [f], X.P. Huang [a], X.B. Ji [a], Q.Y. Jia [j], C.H. Jiang [a], X.S. Jiang [a], D.P. Jin [a], S. Jin [a], Y. Jin [a], Y.F. Lai [a], F. Li [a], G. Li [a], H.H. Li [a], J. Li [a], J.C. Li [a], Q.J. Li [a], R.B. Li [a], R.Y. Li [a], S.M. Li [a], W.G. Li [a], X.L. Li [g], X.Q. Li [i], X.S. Li [n], Y.F. Liang [m], H.B. Liao [e], C.X. Liu [a], F. Liu [e], Fang Liu [o], H.M. Liu [a], J.B. Liu [a], J.P. Liu [p], R.G. Liu [a], Z.A. Liu [a], Z.X. Liu [a], F. Lu [a], G.R. Lu [d], J.G. Lu [a], C.L. Luo [h], X.L. Luo [a], F.C. Ma [g], J.M. Ma [a], L.L. Ma [k], Q.M. Ma [a], X.Y. Ma [a], Z.P. Mao [a], X.H. Mo [a], J. Nie [a], Z.D. Nie [a], H.P. Peng [o], N.D. Qi [a], C.D. Qian [l], H. Qin [h], J.F. Qiu [a], Z.Y. Ren [a], G. Rong [a], L.Y. Shan [a], L. Shang [a], D.L. Shen [a], X.Y. Shen [a], H.Y. Sheng [a], F. Shi [a], X. Shi [j], H.S. Sun [a], S.S. Sun [o], Y.Z. Sun [a], Z.J. Sun [a], X. Tang [a], N. Tao [o], Y.R. Tian [n], G.L. Tong [a], D.Y. Wang [a], J.Z. Wang [a], K. Wang [o], L. Wang [a], L.S. Wang [a], M. Wang [a], P. Wang [a], P.L. Wang [a], S.Z. Wang [a], W.F. Wang [a], Y.F. Wang [a], Zhe Wang [a], Z. Wang [a], Zheng Wang [a], Z.Y. Wang [a], C.L. Wei [a], D.H. Wei [c], N. Wu [a], Y.M. Wu [a], X.M. Xia [a], X.X. Xie [a], B. Xin [g], G.F. Xu [a], H. Xu [a], Y. Xu [a], S.T. Xue [a], M.L. Yan [o], F. Yang [i], H.X. Yang [a], J. Yang [o], S.D. Yang [a], Y.X. Yang [c], M. Ye [a], M.H. Ye [b], Y.X. Ye [o], L.H. Yi [f], Z.Y. Yi [a], C.S. Yu [a], G.W. Yu [a], C.Z. Yuan [a], J.M. Yuan [a], Y. Yuan [a], Q. Yue [a], S.L. Zang [a], Yu. Zeng [a], Y. Zeng [f], B.X. Zhang [a], B.Y. Zhang [a], C.C. Zhang [a], D.H. Zhang [a], H.Y. Zhang [a], J. Zhang [a], J.Y. Zhang [a], J.W. Zhang [a], L.S. Zhang [a], Q.J. Zhang [a], S.Q. Zhang [a], X.M. Zhang [a], X.Y. Zhang [k], Y.J. Zhang [j], Y.Y. Zhang [a], Yiyun Zhang [m], Z.P. Zhang [o], Z.Q. Zhang [d], D.X. Zhao [a], J.B. Zhao [a], J.W. Zhao [a], M.G. Zhao [i], P.P. Zhao [a], W.R. Zhao [a], X.J. Zhao [a], Y.B. Zhao [a],

doi:10.1016/j.physletb.2004.07.004

H.Q. Zheng [j], J.P. Zheng [a], L.S. Zheng [a], Z.P. Zheng [a], X.C. Zhong [a], B.Q. Zhou [a], G.M. Zhou [a], L. Zhou [a], N.F. Zhou [a], K.J. Zhu [a], Q.M. Zhu [a], Y.C. Zhu [a], Y.S. Zhu [a], Yingchun Zhu [a], Z.A. Zhu [a], B.A. Zhuang [a], B.S. Zou [a]

[a] *Institute of High Energy Physics, Beijing 100039, People's Republic of China*
[b] *China Center for Advanced Science and Technology, Beijing 100080, People's Republic of China*
[c] *Guangxi Normal University, Guilin 541004, People's Republic of China*
[d] *Henan Normal University, Xinxiang 453002, People's Republic of China*
[e] *Huazhong Normal University, Wuhan 430079, People's Republic of China*
[f] *Hunan University, Changsha 410082, People's Republic of China*
[g] *Liaoning University, Shenyang 110036, People's Republic of China*
[h] *Nanjing Normal University, Nanjing 210097, People's Republic of China*
[i] *Nankai University, Tianjin 300071, People's Republic of China*
[j] *Peking University, Beijing 100871, People's Republic of China*
[k] *Shandong University, Jinan 250100, People's Republic of China*
[l] *Shanghai Jiaotong University, Shanghai 200030, People's Republic of China*
[m] *Sichuan University, Chengdu 610064, People's Republic of China*
[n] *Tsinghua University, Beijing 100084, People's Republic of China*
[o] *University of Science and Technology of China, Hefei 230026, People's Republic of China*
[p] *Wuhan University, Wuhan 430072, People's Republic of China*
[q] *Zhejiang University, Hangzhou 310028, People's Republic of China*

Received 10 June 2004; accepted 5 July 2004

Available online 23 July 2004

Editor: M. Doser

Abstract

The absolute branching fractions for the decays $D^0 \to K^- e^+ \nu_e$ and $D^0 \to \pi^- e^+ \nu_e$ are determined using $7584 \pm 198 \pm 341$ singly tagged $\bar{D}^0$ sample from the data collected around 3.773 GeV with the BES-II detector at the BEPC. In the system recoiling against the singly tagged $\bar{D}^0$ meson, 104.0 ± 10.9 events for $D^0 \to K^- e^+ \nu_e$ and 9.0 ± 3.6 events for $D^0 \to \pi^- e^+ \nu_e$ decays are observed. Those yield the absolute branching fractions to be $BF(D^0 \to K^- e^+ \nu_e) = (3.82 \pm 0.40 \pm 0.27)\%$ and $BF(D^0 \to \pi^- e^+ \nu_e) = (0.33 \pm 0.13 \pm 0.03)\%$. The vector form factors are determined to be $|f_+^K(0)| = 0.78 \pm 0.04 \pm 0.03$ and $|f_+^\pi(0)| = 0.73 \pm 0.14 \pm 0.06$. The ratio of the two form factors is measured to be $|f_+^\pi(0)/f_+^K(0)| = 0.93 \pm 0.19 \pm 0.07$.

1. Introduction

The semileptonic decays of the charmed mesons are theoretically simplest to interpret because the effects of the weak and strong interactions can be well separated. The decay amplitude is proportional to the product of the Cabibbo–Kobayashi–Maskawa (CKM) matrix element, which parametrizes the mixing between the quark mass eigenstates and the weak eigenstates, and the form factor describing the strong interaction between the final state quarks. The differential decay rate for $D^0 \to K^-(\pi^-)e^+\nu_e$ process is described by

$$\frac{d\Gamma}{dq^2} = \frac{G_F^2}{24\pi^3}|V_{cs(d)}|^2 \mathbf{p}_{K(\pi)}^3 \left| f_+^{K(\pi)}(q^2) \right|^2, \tag{1}$$

where G_F is the Fermi coupling constant, $|V_{cs(d)}|$ is the CKM matrix element and $\mathbf{p}_{K(\pi)}$ is the momentum of the kaon (pion) in the rest frame of the D^0 meson. $f_+^{K(\pi)}(q^2)$ represents the vector form factor of the hadronic weak current depending on the square of the four momentum transfer $q = p_D - p_{K(\pi)}$. In general theoretical treatment one common form of the form

E-mail address: rongg@mail.ihep.ac.cn (G. Rong).

factor is a single pole form and is expressed as

$$f_+(q^2) = \frac{f_+(0)}{1 - q^2/m_*^2}, \quad (2)$$

where $f_+(0)$ is the form factor evaluated at the four momentum transfer q equal to zero, and the pole mass m_* is the mass of the lowest-lying $Q\bar{q}'$ meson.

MARKIII [1] previously made an absolute measurements of the branching fractions for $D^0 \to K^- e^+ \nu_e$ and $D^0 \to \pi^- e^+ \nu_e$ by analysing the data taken at the near $D\bar{D}$ threshold region. In this Letter, we report the direct measurements of the branching fractions for the Cabibbo favored decay of $D^0 \to K^- e^+ \nu_e$ (throughout this Letter, charged conjugation is implied) and the Cabibbo suppressed decay of $D^0 \to \pi^- e^+ \nu_e$ by analysing the data sample of integrated luminosity of 33 pb^{-1} collected at and around the center of mass energy of 3.773 GeV with the BES-II detector at the BEPC. Using the measured branching fractions, the well measured $|V_{cs}|$, $|V_{cd}|$ and the lifetime of the D^0 meson quoted from PDG [2], the vector form factors $|f_+^\pi(0)|$ and $|f_+^K(0)|$ are extracted, and their ratio is determined directly.

2. BES-II detector

BES-II is a conventional cylindrical magnetic detector that is described in detail in Ref. [3]. A 12-layer vertex chamber (VC) surrounding the beryllium beam pipe provides input to the event trigger, as well as coordinate information. A forty-layer main drift chamber (MDC) located just outside the VC yields precise measurements of charged particle trajectories with a solid angle coverage of 85% of 4π; it also provides ionization energy loss (dE/dx) measurements which are used for particle identification. Momentum resolution of $1.7\%\sqrt{1+p^2}$ (p in GeV/c) and dE/dx resolution of 8.5% for Bhabha scattering electrons are obtained for the data taken at $\sqrt{s} = 3.773$ GeV. An array of 48 scintillation counters surrounding the MDC measures the time of flight (TOF) of charged particles with a resolution of about 180 ps for electrons. Outside the TOF, a 12 radiation length, lead-gas barrel shower counter (BSC), operating in limited streamer mode, measures the energies of electrons and photons over 80% of the total solid angle with an energy resolution of $\sigma_E/E = 0.22/\sqrt{E}$ (E in GeV) and spatial resolutions of $\sigma_\phi = 7.9$ mrad and $\sigma_Z = 2.3$ cm for electrons. A solenoidal magnet outside the BSC provides a 0.4 T magnetic field in the central tracking region of the detector. Three double-layer muon counters instrument the magnet flux return, and serve to identify muons of momentum greater than 500 MeV/c. They cover 68% of the total solid angle.

3. Data analysis

At the center of mass energies around 3.773 GeV, the $\psi(3770)$ resonance is produced in electron–positron (e^+e^-) annihilation. The $\psi(3770)$ decays predominately into $D\bar{D}$ pairs. If one D meson is fully reconstructed, the anti-D meson must exist in the system recoiling against the fully reconstructed D meson (called singly tagged D). Using the singly tagged $\bar{D}^0$ sample, the decays of $D^0 \to K^- e^+ \nu_e$ and $D^0 \to \pi^- e^+ \nu_e$ can be well selected in the recoiling system. Therefore, the absolute branching fractions for these decays can be well measured.

3.1. Event selection

The $\bar{D}^0$ meson is reconstructed in non-leptonic decay modes of $K^+\pi^-$, $K^+\pi^-\pi^-\pi^+$, $K^0\pi^+\pi^-$ and $K^+\pi^-\pi^0$. Events which contain at least two reconstructed charged tracks with good helix fits are selected. In order to ensure the well-measured 3-momentum vectors and the reliable charged-particle identification, the charged tracks used in the single tag analysis are required to be within $|\cos\theta| < 0.85$ where θ is the polar angle. All tracks, save those from K_S^0 decays, must originate from the interaction region, which require that the closest approach of a charged track in xy plane is less than 2.0 cm and the z position of the charged track is less than 20.0 cm. Pions and kaons are identified by means of TOF and dE/dx measurements. Pion identification requires a consistency with the pion hypothesis at a confidence level (CL_π) greater than 0.1%. In order to reduce misidentification, a kaon candidate is required to have a larger confidence level (CL_K) for a kaon hypothesis than that for a pion hypothesis. For electron identification, the combined confidence level (CL_e), calculated for the e hypothesis using the dE/dx, TOF and BSC mea-

surements, is required to be greater than 0.1%, and the ratio $CL_e/(CL_e + CL_\pi + CL_K)$ is required to be greater than 0.8. The π^0 is reconstructed in the decay of $\pi^0 \to \gamma\gamma$. To select good photons from the decay of π^0, the energy of a photon deposited in the BSC is required to be greater than 0.07 GeV, and the electromagnetic shower is required to start in the first 5 readout layers. In order to reduce the backgrounds the angle between the photon and the nearest charged track is required to be greater than 22° and the angle between the direction of the cluster development and the direction of the photon emission to be less than 37°.

3.2. Singly tagged $\bar{D}^0$ sample

For each event, there may be several different charged track (or charged and neutral track) combinations for each of the four single tag modes. Each combination is subject to a center-of-mass energy constraint kinematic fit and is required to have a fit probability $P(\chi^2)$ greater than 0.1%. If more than one combination satisfies $P(\chi^2) > 0.1\%$, the combination with the largest fit probability is retained. For the single tag modes with a neutral kaon and/or neutral pion, one additional constraint kinematic fit for the $K^0_S \to \pi^+\pi^-$ and/or $\pi^0 \to \gamma\gamma$ hypothesis is performed, separately.

The resulting distributions in the fitted invariant masses of $Kn\pi$ $(n = 1, 2, 3)$ combinations, which are calculated using the fitted momentum vectors from the kinematic fit, are shown in Fig. 1. The signals for the singly tagged $\bar{D}^0$ are clearly observed in the fitted mass spectra. A maximum likelihood fit to the mass spectrum with a Gaussian function for the $\bar{D}^0$ signal and a special background function[1] to describe backgrounds yields the number of the singly tagged $\bar{D}^0$ events for each of the four modes and the total number of $7584 \pm 198 \pm 341$ reconstructed $\bar{D}^0$ mesons. The first error is statistical; the second error is systematic and is obtained by varying the parameterization of the background.

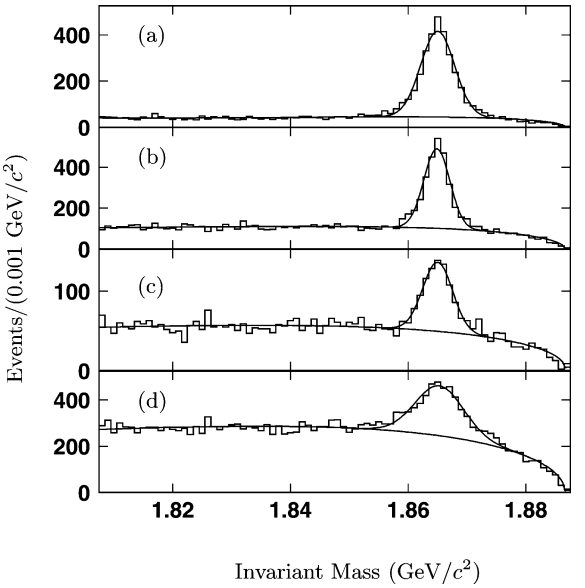

Fig. 1. Distributions of the fitted invariant masses of (a) $K^+\pi^-$, (b) $K^+\pi^-\pi^+\pi^-$, (c) $K^0_S\pi^+\pi^-$ and (d) $K^+\pi^-\pi^0$ combinations.

3.3. Candidates of $D^0 \to K^-e^+\nu_e$ and $D^0 \to \pi^-e^+\nu_e$

Candidate events $D^0 \to K^-e^+\nu_e$ and $D^0 \to \pi^-e^+\nu_e$ are selected from the surviving tracks in the system recoiling against the tagged $\bar{D}^0$. To select the $D^0 \to K^-e^+\nu_e$ and $D^0 \to \pi^-e^+\nu_e$ events, it is required that there are only two oppositely charged tracks, one of which is identified as an electron and the other as a kaon or pion. The neutrino is undetected, therefore the kinematic quantity $U_{\rm miss} \equiv E_{\rm miss} - p_{\rm miss}$ is used to obtain the information about the missing neutrino, where $E_{\rm miss}$ and $p_{\rm miss}$ are the missing energy and the missing momentum, respectively, which are carried by the undetected particles. Fig. 2(a) and (b) show the $U_{\rm miss}$ distributions for the Monte Carlo $D^0 \to K^-e^+\nu_e$ and $D^0 \to \pi^-e^+\nu_e$ events,

[1] A Gaussian function was assumed for the signal. The background shape was

$$(1.0 + p_1 y + p_2 y^2) N \sqrt{1 - \left(\frac{x}{E_b}\right)^2}\, e^{-f(1-x/E_b)^2},$$

where $N\sqrt{1-(x/E_b)^2}e^{-f(1-x/E_b)^2}$ is ARGUS background shape, the x is the fitted mass, E_b is the beam energy, $y = (E_b - x)/(E_b - 1.8)$, N, f, p_1 and p_2 are the fit parameters. The ARGUS background shape was used by ARGUS experiment to parametrize the background for fitting B mass peaks. For detail, see: Ian C. Brock, Mn-Fit, a fitting and plotting package using MINUIT, Version 4.07, December 22, 2000.

respectively. The candidate events are required to satisfy the requirement $|U_{\rm miss}| < 3\sigma_{U_{\rm miss}}$, where the $\sigma_{U_{\rm miss}}$ is the standard deviation of the $U_{\rm miss}$ distribution.

The branching fraction of the Cabibbo favored decay $D^0 \to K^- e^+ \nu_e$ is much larger than that of the Cabibbo suppressed decay $D^0 \to \pi^- e^+ \nu_e$. The kaon can be misidentified as pion and therefore the process $D^0 \to K^- e^+ \nu_e$ in the recoil side can be misclassified as $D^0 \to \pi^- e^+ \nu_e$. Monte Carlo study shows that this decay process is the main contamination to the selected sample of $D^0 \to \pi^- e^+ \nu_e$ process. In order to correctly select the events $D^0 \to \pi^- e^+ \nu_e$ and suppress misidentification from $D^0 \to K^- e^+ \nu_e$, the quantity $U_{\pi\text{-as-}K}$ is calculated by replacing pion mass with the kaon mass and $|U_{\rm miss}| < |U_{\pi\text{-as-}K}|$ is required. Fig. 2(c) shows the $U_{\rm miss}$ calculated by replacing pion mass with kaon mass for the Monte Carlo events of $D^0 \to \pi^- e^+ \nu_e$, while Fig. 2(d) shows the distributions of $U_{\rm miss}$ calculated by replacing kaon mass with pion mass for the Monte Carlo events of $D^0 \to K^- e^+ \nu_e$. The quantity $U_{\rm miss}$ is expected to be closer to zero for the correct particle mass assignment. The decays such as $D^0 \to K^- \pi^0 e^+ (\mu^+) \nu_e (\nu_\mu)$ are suppressed by rejecting the events with extra isolated photons which are not used in the reconstruction of the singly tagged $\bar{D}^0$. The isolated photon should have its energy greater than 0.1 GeV and satisfy photon selection criteria as mentioned earlier.

Fig. 3(a) and (b) show the distributions of the fitted invariant masses of the $Kn\pi$ combinations for the events in which the $D^0 \to K^- e^+ \nu_e$ and $D^0 \to \pi^- e^+ \nu_e$ candidate events are observed in the system recoiling against the singly tagged $\bar{D}^0$. In Fig. 3(a), there are 118 events in $\pm 3\sigma$ signal regions, while there are 10 events in the outside of the signal regions. By assuming that the background distribution is flat, 3.8 ± 1.3 background events are estimated in the signal region. After subtracting the number of background events in the signal region, 114.2 ± 10.9 candidate events are retained. A similar analysis of the events in Fig. 3(b) gives that there are 11.0 ± 3.6 candidate events after subtracting the number of background events in the signal region.

Fig. 4(a) and (b) show distributions of the $U_{\rm miss}$ calculated for the selected events of $D^0 \to K^- e^+ \nu_e$ and $D^0 \to \pi^- e^+ \nu_e$, respectively. Fig. 5 shows distribution of the momentum of the electrons from the selected

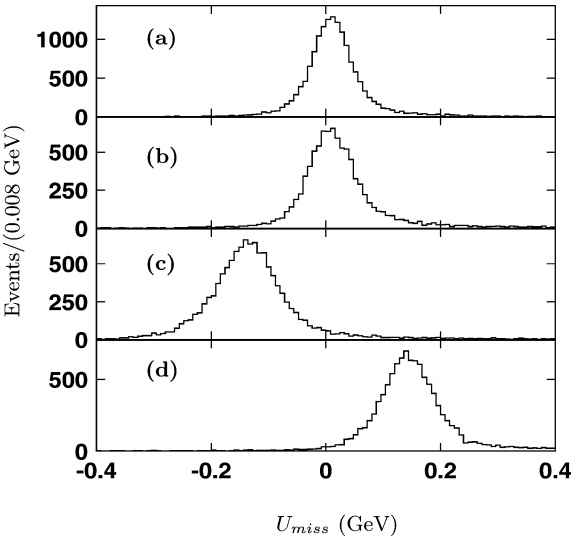

Fig. 2. Distribution of $U_{\rm miss}$ calculated for the Monte Carlo events of (a) $D^0 \to K^- e^+ \nu_e$, (b) $D^0 \to \pi^- e^+ \nu_e$, (c) $D^0 \to \pi^- e^+ \nu_e$ by replacing pion mass with kaon mass and (d) $D^0 \to K^- e^+ \nu_e$ by replacing kaon mass with pion mass.

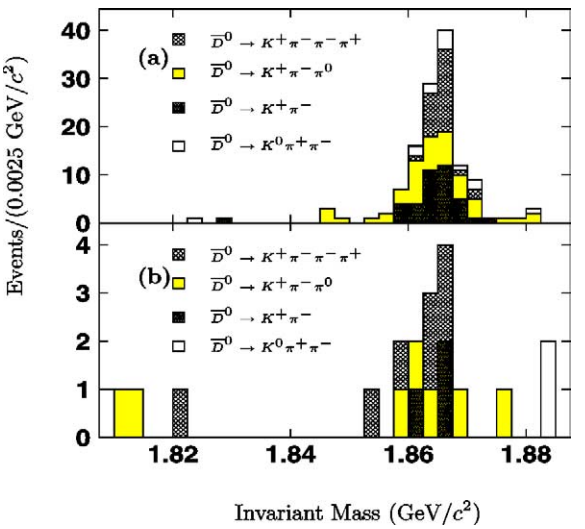

Fig. 3. Distributions of the fitted invariant masses of $Kn\pi$ combinations for the events in which (a) the $D^0 \to K^- e^+ \nu_e$ and (b) the $D^0 \to \pi^- e^+ \nu_e$ candidate events are observed in the system recoiling against the tagged $\bar{D}^0$.

candidate events of $D^0 \to K^- e^+ \nu_e$, where the error bars are for the events from the data and the histogram is for the events of $D^0 \to K^- e^+ \nu_e$ from Monte Carlo sample.

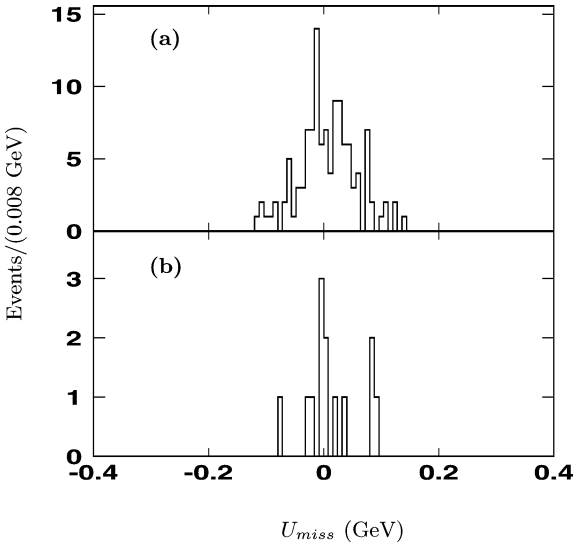

Fig. 4. Distribution of $U_{\rm miss}$ calculated for the selected candidate events of (a) $D^0 \to K^- e^+ \nu_e$ and (b) $D^0 \to \pi^- e^+ \nu_e$.

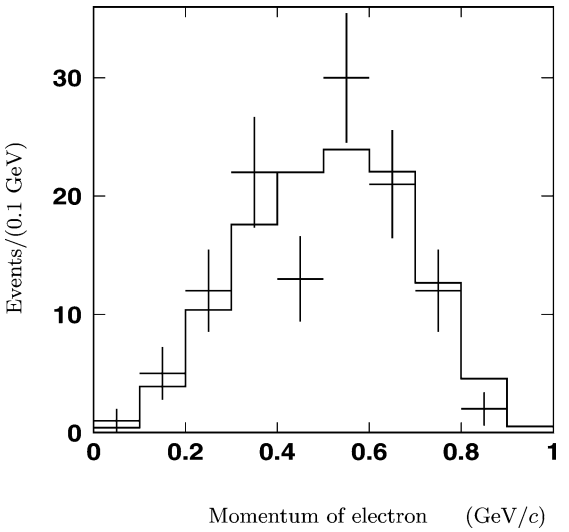

Fig. 5. Distribution of the momentum of the electrons from the selected candidate events of $D^0 \to K^- e^+ \nu_e$, where the error bars are for the events from the data and the histogram is for the events of $D^0 \to K^- e^+ \nu_e$ from Monte Carlo sample.

3.4. Background subtraction

There are still some background contaminations in the observed candidate events due to other semileptonic or hadronic decays. These background events must be subtracted from the candidate events. The numbers of background are estimated by analysing the Monte Carlo sample which is 13 times larger than the data. The Monte Carlo events are generated as $e^+e^- \to D\bar{D}$ and the D and $\bar{D}$ mesons are set to decay to all possible final states according to the decay modes and branching fractions quoted from PDG [2] except the two decay modes under study. The number of events satisfying the selection criteria is then renormalized to the corresponding data set. Totally 10.2 ± 1.0 and 2.0 ± 0.5 background events are obtained for $D^0 \to K^- e^+ \nu_e$ and $D^0 \to \pi^- e^+ \nu_e$, respectively. After subtracting these numbers of background events, 104.0 ± 10.9 and 9.0 ± 3.6 signal events for $D^0 \to K^- e^+ \nu_e$ and $D^0 \to \pi^- e^+ \nu_e$ decays are retained.

4. Results

4.1. Monte Carlo efficiency

The efficiencies for reconstruction of the semileptonic decay events of $D^0 \to K^- e^+ \nu_e$ and $D^0 \to \pi^- e^+ \nu_e$ are estimated by Monte Carlo simulation. A detailed Monte Carlo study shows that the efficiencies are $\epsilon_{K^- e^+ \nu_e} = (35.89 \pm 0.25)\%$ and $\epsilon_{\pi^- e^+ \nu_e} = (36.02 \pm 0.25)\%$, where the errors are statistical.

4.2. Branching fractions

The measured branching fractions are obtained by dividing the observed numbers of the semileptonic decay events $N(D^0 \to K^-(\pi^-)e^+\nu_e)$ by the number of the singly tagged $\bar{D}^0$ meson $N_{\bar{D}^0_{\rm tag}}$ and the reconstruction efficiencies $\epsilon_{K^- e^+ \nu_e(\pi^- e^+ \nu_e)}$,

$$Br\big(D^0 \to K^-(\pi^-)e^+\nu_e\big) = \frac{N(D^0 \to K^-(\pi^-)e^+\nu_e)}{\epsilon_{K^- e^+ \nu_e(\pi^- e^+ \nu_e)} N_{\bar{D}^0_{\rm tag}}}. \quad (3)$$

Inserting these numbers into Eq. (3), the branching fractions for $D^0 \to K^- e^+ \nu_e$ and $D^0 \to \pi^- e^+ \nu_e$ decays are obtained to be

$$BF\big(D^0 \to K^- e^+ \nu_e\big) = (3.82 \pm 0.40 \pm 0.27)\%$$

and

$$BF\big(D^0 \to \pi^- e^+ \nu_e\big) = (0.33 \pm 0.13 \pm 0.03)\%,$$

where the first errors are statistical and the second systematic. The systematic uncertainties in the measured branching fractions arise from the uncertainties of particle identification (1.1%), tracking efficiency (2.0% per track), photon reconstruction (2.0%), $U_{\rm miss}$ selection (0.6% for $D^0 \to K^- e^+ \nu_e$, 1.2% for $D^0 \to \pi^- e^+ \nu_e$), the number of the singly tagged $\bar{D}^0$ (4.8%), background subtraction (2.3% for $D^0 \to K^- e^+ \nu_e$, 5.6% for $D^0 \to \pi^- e^+ \nu_e$) and Monte Carlo statistics (0.8%). These uncertainties are added in quadrature to obtain the total systematic errors, which are 7.1% and 8.8% for $D^0 \to K^- e^+ \nu_e$ and $D^0 \to \pi^- e^+ \nu_e$, respectively.

4.3. Form factors $|f_+^K(0)|$ and $|f_+^\pi(0)|$

The decay width [7,8] of the semileptonic decay processes can be derived from Eq. (1) by substituting the single pole form of the form factor as given in Eq. (2) for $|f_+^{K(\pi)}(q^2)|$ in Eq. (1). The relations between the decay widths and the form factors are

$$\Gamma\left(D^0 \to K^- e^+ \nu_e\right) = 1.53|V_{cs}|^2 \left|f_+^K(0)\right|^2 \times 10^{11}\ \mathrm{s}^{-1}, \quad (4)$$

$$\Gamma\left(D^0 \to \pi^- e^+ \nu_e\right) = 3.01|V_{cd}|^2 \left|f_+^\pi(0)\right|^2 \times 10^{11}\ \mathrm{s}^{-1}. \quad (5)$$

The form factors $|f_+^K(0)|$ and $|f_+^\pi(0)|$ can be extracted by using the measured values of the branching fractions and the lifetime of the D^0 meson. Inserting the values of $|V_{cs}| = 0.996 \pm 0.013$, $|V_{cd}| = 0.224 \pm 0.016$ and the lifetime $\tau_{D^0} = (411.7 \pm 2.7) \times 10^{-15}$ s into Eqs. (4) and (5), the form factors are obtained to be

$$\left|f_+^K(0)\right| = 0.78 \pm 0.04 \pm 0.03,$$
$$\left|f_+^\pi(0)\right| = 0.73 \pm 0.14 \pm 0.06,$$

where the first errors are statistical and the second are systematic errors which arise from the systematic uncertainties in the measured values of the branching fractions, the uncertainties in the values of $|V_{cs}|$, $|V_{cd}|$ and τ_{D^0}. The values of the form factors are compared with that predicted by various theoretical models and enumerated in Table 1. The ratio of the two form factors can be obtained from Eqs. (3), (4) and (5),

$$\frac{|f_+^\pi(0)|}{|f_+^K(0)|} = 0.71 \frac{|V_{cs}|}{|V_{cd}|} \sqrt{\frac{N(D^0 \to \pi^- e^+ \nu_e)\epsilon_{K^- e^+ \nu_e}}{N(D^0 \to K^- e^+ \nu_e)\epsilon_{\pi^- e^+ \nu_e}}}, \quad (6)$$

Inserting the $|V_{cd}|$, $|V_{cs}|$, the numbers of the signal events and the efficiencies into Eq. (6), the value of the ratio is obtained. It is

$$\left|\frac{f_+^\pi(0)}{f_+^K(0)}\right| = 0.93 \pm 0.19 \pm 0.07,$$

where the first error is statistical and the second systematic which arises from the systematic uncertainties in the measured values of the branching fractions and the uncertainties in the values of $|V_{cs}|$ and $|V_{cd}|$. This result is consistent with theoretical predictions, which range from 0.7 to 1.4 [9].

4.4. CKM matrix elements $|V_{cs}|$ and $|V_{cd}|$

Reversing the argument that is presented in the previous section, we obtain the measured values of the CKM matrix elements $|V_{cs}|$ and $|V_{cd}|$ using the predicted form factors as shown in Table 1. The results are listed in Table 2. As a comparison, the values of

Table 1
Form factors

	$\left\|f_+^K(0)\right\|$	$\left\|f_+^\pi(0)\right\|$
QCDSR [4]	0.78 ± 0.11	0.65 ± 0.11
LQCD1 [5]	$0.71 \pm 0.03^{+0.00}_{-0.07}$	$0.64 \pm 0.05^{+0.00}_{-0.07}$
LQCD2 [6]	$0.66 \pm 0.04^{+0.01}_{-0.00}$	$0.57 \pm 0.06^{+0.01}_{-0.00}$
BES	$0.78 \pm 0.04 \pm 0.03$	$0.73 \pm 0.14 \pm 0.06$

Table 2
CKM matrix elements

$\|V_{cs}\|$	$\|V_{cd}\|$	$f_+^{K(\pi)}(0)$ input
$0.998 \pm 0.052 \pm 0.145$	$0.251 \pm 0.049 \pm 0.044$	QCDSR [4]
$1.097 \pm 0.057^{+0.061}_{-0.124}$	$0.255 \pm 0.050^{+0.023}_{-0.036}$	LQCD1 [5]
$1.180 \pm 0.062^{+0.085}_{-0.083}$	$0.286 \pm 0.056^{+0.033}_{-0.033}$	LQCD2 [6]
0.996 ± 0.013	0.224 ± 0.016	PDG

Table 3
The ratio of the CKM matrix elements

	BES	MARKIII [1]
$\|V_{cd}/V_{cs}\|^2$	$0.043 \pm 0.017 \pm 0.003$	$0.057^{+0.038}_{-0.015} \pm 0.005$

the CKM matrix elements quoted from PDG [2] are also listed in Table 2.

Finally, Table 3 gives the comparison of the ratio of the CKM matrix elements with that obtained by MARKIII, in which the ratio of the form factors is taken to be unity.

5. Summary

In summary, by analysing the data collected at and around 3.773 GeV with the BES-II detector at the BEPC, the branching fractions for the decay of $D^0 \to K^- e^+ \nu_e$ and $D^0 \to \pi^- e^+ \nu_e$ have been measured. From a total of $7584 \pm 198 \pm 341$ singly tagged $\bar{D}^0$ events, 104.0 ± 10.9 $D^0 \to K^- e^+ \nu_e$ and 9.0 ± 3.6 $D^0 \to \pi^- e^+ \nu_e$ signal events are observed in the system recoiling against the $\bar{D}^0$ tags. Those yield the decay branching fractions to be $BF(D^0 \to K^- e^+ \nu_e) = (3.82 \pm 0.40 \pm 0.27)\%$ and $BF(D^0 \to \pi^- e^+ \nu_e) = (0.33 \pm 0.13 \pm 0.03)\%$. Using the values of the CKM matrix elements quoted from PDG [2], the form factors $|f_+^K(0)|$ and $|f_+^\pi(0)|$ are determined to be $|f_+^K(0)| = 0.78 \pm 0.04 \pm 0.03$, $|f_+^\pi(0)| = 0.73 \pm 0.14 \pm 0.06$ and the ratio of the two form factor to be $|f_+^\pi(0)/f_+^K(0)| = 0.93 \pm 0.19 \pm 0.07$. In addition, using the form factors predicted by QCDSR and LQCD calculations, the CKM matrix elements $|V_{cs}|$ and $|V_{cd}|$ are also determined.

Acknowledgements

The BES Collaboration thanks the staff of BEPC for their hard efforts. This work is supported in part by the National Natural Science Foundation of China under contracts Nos. 19991480, 10225524, 10225525, the Chinese Academy of Sciences under contract No. KJ 95T-03, the 100 Talents Program of CAS under contract Nos. U-11, U-24, U-25, and the Knowledge Innovation Project of CAS under contract Nos. U-602, U-34 (IHEP); by the National Natural Science Foundation of China under Contract No. 10175060 (USTC), and No. 10225522 (Tsinghua University).

References

[1] MarkIII Collaboration, J. Adler, et al., Phys. Rev. Lett. 62 (1989) 1821;
Z. Bai, et al., Phys. Rev. Lett. 66 (1991) 1011.
[2] Particle Data Group, Phys. Rev. D 66 (2002) 010001.
[3] BES Collaboration, J.Z. Bai, et al., Nucl. Instrum. Methods A 458 (2001) 627.
[4] A. Khodjamirian, et al., Phys. Rev. D 62 (2000) 114002.
[5] A. Abada, et al., Nucl. Phys. B (Proc. Suppl.) 83 (2000) 286.
[6] A. Abada, et al., Nucl. Phys. B 619 (2001) 565.
[7] R.J. Morrison, M.S. Witherell, Annu. Rev. Part. Sci. 39 (1989) 183.
[8] M. Ablikim, J.C. Chen, G. Rong, D.H. Zhang, The Cabibbo suppressed semileptonic decay $D^0 \to \pi^- e^+ \nu_e$, High Energy Phys. Nucl. Phys., submitted for publication.
[9] J.D. Richman, P.R. Burchat, Rev. Mod. Phys. 67 (4) (1995).